

## Influence of ZnO on Antibacterial Properties of Portland Cement

Rahadian Zainul<sup>a,b,\*</sup>, Randy Trafino<sup>b</sup>, Krismadinata<sup>a,c</sup>, Remon Lapisa<sup>a,d</sup>, Putri Azhari<sup>e</sup>, Amalia Putri Lubis<sup>b</sup>, Muhardi<sup>f</sup>

<sup>a</sup> Center for Energy and Power Electronics Research (CEPER), Universitas Negeri Padang, Padang, West Sumatera, Indonesia

<sup>b</sup> Department of Chemistry, Universitas Negeri Padang, Padang, West Sumatera, Indonesia

<sup>c</sup> Department of Electrical Engineering, Faculty of Engineering, Universitas Negeri Padang, Padang, West Sumatera, Indonesia

<sup>d</sup> Department of Mechanical Engineering, Faculty of Engineering, Universitas Negeri Padang, Padang, West Sumatera, Indonesia

<sup>e</sup> Department of Agricultural Technology, Faculty of Agricultural Technology, Andalas University, Padang, West Sumatera, Indonesia

<sup>f</sup> Informatics Engineering Study Program, Faculty of Computer Science, Hang Tuah University, Pekanbaru, Riau, Indonesia

Corresponding author: \*rahadianzmsiphd@gmail.com

**Abstract**— This research project focuses on evaluating the antimicrobial properties of a composite material composed of Portland Cement and Zinc Oxide (ZnO). The study assesses the antibacterial activity of this composite by using *Escherichia coli* (E. coli) as the test microorganism. Bacterial growth assessment is carried out through the Total Plate Count (TPC) method. The investigation involved varying the concentration of ZnO within the Portland Cement composite, specifically at levels of 0%, 1%, 3%, and 5%. The study primarily centers on generating reactive oxygen species (ROS) by ZnO, and this evaluation was conducted under both UV light exposure and without it. This dual approach allows for a comprehensive examination of ROS activity. Furthermore, the research project involves material characterization using X-ray Diffraction (XRD) to determine the nanoparticle size of ZnO and identify the crystal structures present within the composite material. Additionally, morphological analysis is performed using Scanning Electron Microscopy (SEM) to visualize the structural properties of ZnO embedded within the Portland Cement. SEM analysis is conducted at various magnifications, including 1000x, 2500x, 5000x, and 10,000x, to provide a detailed view of the ZnO's structural properties. In summary, this research project explores the antimicrobial potential of a composite material incorporating Portland Cement and ZnO, focusing on ROS generation and the composite material's structural properties. The findings will contribute to our understanding of the material's suitability for applications in antimicrobial environments.

**Keywords**— Portland cement; ZnO; *Escherichia coli*; antibacterial; total plate count.

Manuscript received 10 Jul. 2023; revised 21 Sep. 2023; accepted 8 Nov. 2023. Date of publication 31 Dec. 2023.  
IJASEIT is licensed under a Creative Commons Attribution-Share Alike 4.0 International License.



### I. INTRODUCTION

Composite cement production, used to make cement mortar and concrete, is one of the most significant branches in the building materials industry today. Nanoparticles are used in electronics, cosmetics, the food industry, agriculture, and building materials (especially those made from composite cement). One form of composite cement is Portland cement [1], [2]. The basic ingredients of cement are divided into three types, namely clinker 70%-95%, which is the result of burning limestone, silica sand, iron sand, and clay, then about 5% gypsum is used as a retarder, and third material, such as limestone, pozzolan, fly ash, etc. [3], [4].

Portland cement is made in several stages; the first is limestone/coral obtained in the coal firing process, broken down to a size of < 50mm. The second is limestone tested with

a predetermined size mixed with clay, sand, and iron ore. In the third process, after mixing, the results are brought to the ball mill and mixed with water, and then a concentrated solution with a texture-like texture is formed. In the usual slurry, in the fourth process, testing is carried out according to specifications.

TABLE I  
COMPOUNDS CONTAINED IN PORTLAND CEMENT [7]

Chemical Properties	Percentage (%)
Loss on Ignition	2.05
Insoluble Residue	4.10
Chloride	0.07
SiO <sub>2</sub>	28.7
Al <sub>2</sub> O <sub>3</sub>	13.5
CaO	53.6
MgO	2.21
Fe <sub>2</sub> O <sub>3</sub>	2.27

The last process after testing is carried out by burning the slurry in a rotating kiln with a temperature of 1500°C. Then, clinker, which contains chemical compounds, is produced [5], [6]. The percentage of compounds contained in Portland Cement is in Table 1.

Table 2 shows a notation of Portland cement compounds. However, most cements have a brittle structure, full of capillary cavities, with porous spaces. Because of that, in a period when the weather tends to be challenging to predict, the influence of rainfall and harsh conditions such as normal temperatures allow the cycle of freezing and thawing water

seepage to begin to occur in the cement structure, long-term water intrusion into the cement structure will be accelerated, and the structure gradually decays. In addition to water incursion, moisture left for an extended period on the surface of a cement structure will encourage the growth of bacteria, fungi, and insects. *Escherichia coli* is one of the most prevalent microbiological infections. It spreads, having negative impacts on the environment as well as adverse health conditions such as upper respiratory tract symptoms (cough, sore throat), meningitis, and asthma [9]–[11].

TABLE II  
NOTATION OF PORTLAND CEMENT COMPOUNDS [8]

Oxide	CaO	SiO <sub>2</sub>	Al <sub>2</sub> O <sub>3</sub>	Fe <sub>2</sub> O <sub>3</sub>	K <sub>2</sub> O	MgO	Na <sub>2</sub> O	SO <sub>3</sub>	CO <sub>2</sub>	TiO <sub>2</sub>
Notation	C	S	A	F	K	M	N	S'	C'	T

It is known that ZnO material shows efficiency and better antimicrobial with good photochemical stability. This antimicrobial efficiency is closely related to the superhydrophobicity of ZnO and its high oxidizing power. Reactive oxygen species (ROS) are poisonous and capable of killing bacteria when produced by ZnO in aqueous environments during sun irradiation [12]–[15]. Other benefits or advantages of ZnO are its excellent stability in both acidic and alkaline conditions, biosafety, ecological safety, and relative affordability [16]–[19]. Besides, the antibacterial activity of ZnO nanoparticles has been correlated with its small size and low cost, wide surface-to-volume ratio, encouraging them to interact directly with bacterial membranes [20]–[22]. This research aims to evaluate the antibacterial properties of a Portland Cement composite with varying concentrations of Zinc Oxide, using *E. coli* as a test organism and analyzing the reactive oxygen species' activity, complemented by structural characterization through XRD and SEM.

## II. MATERIAL AND METHODS

### A. Material and Methods

Tools and materials needed are a beaker, measuring cup, analytical balance, stirring rod, dropper pipette, petri dish, filter paper, ultrasonic digital, falcon tube, vortex, ZnO hexahydrate, acetone, Portland cement, *Escherichia coli* bacteria, Aquades, Nutrient Agar and NaOH.

### B. ZnO Synthesis

To synthesize ZnO nanoparticle powder, following the previous procedure with modification [23]. A total of 7 grams of [Zn(NO<sub>3</sub>)<sub>2</sub>.6H<sub>2</sub>O, (Brand, 99.0%)] was dissolved in 117 ml of solution, then added 4 M aqueous solution of NaOH dropwise with constant stirring until it reaches a pH of 12 from which precipitation is reached. Furthermore, after the filtering process, the precipitate formed is washed several times with distilled water, then a few drops of acetone, then a white powder is formed. Then, the white powder was dried in an oven at 110°C for 5 hours.

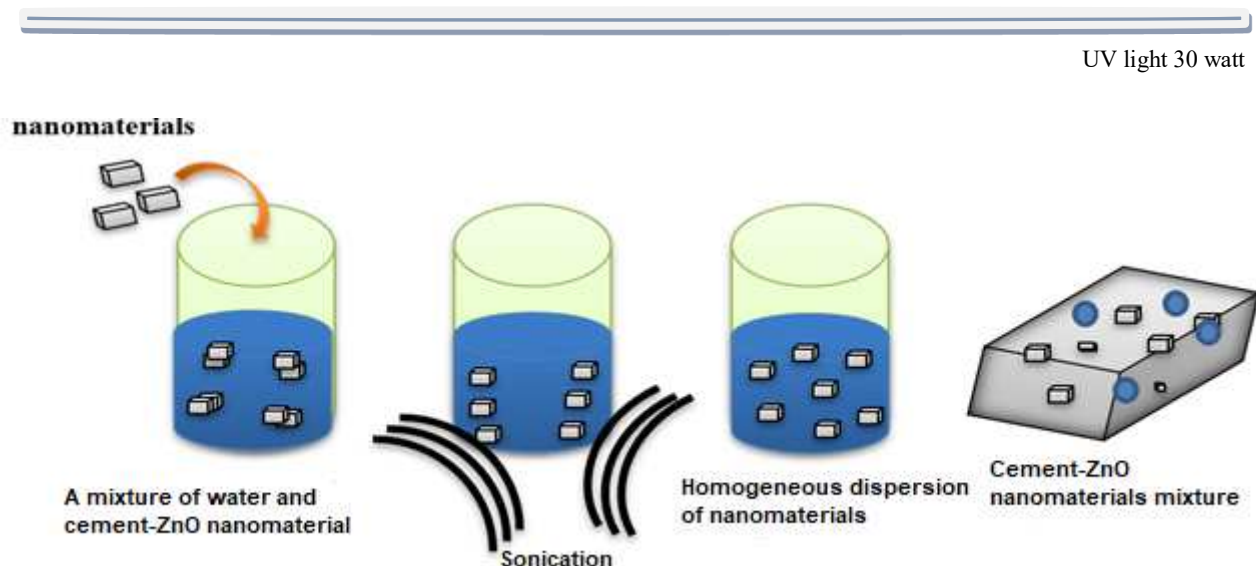


Fig. 1 Schematic process of nanomaterial dispersion methods in the preparation of cement-based composites

White cement and ZnO were mixed tightly utilizing digital ultrasonic technology for two hours under a 30-watt UV light

to achieve uniform mixing. The same procedure was carried out without UV light or the dark [24], [25].

### C. Mixing Process of ZnO powder and Portland Cement

After synthesizing ZnO, ZnO powder was obtained, and four beakers containing cement composite were prepared. ZnO was added in the four composites with variations in 0%, 1%, 3%, and 5% by weight ratio. When making the composite pellets, first combine the ZnO and white cement in the proper quantity, keeping the overall weight of the cement at 1 gram and adding the variation, and then combine with several milliliters of distilled water, which serves as a solvent [26], [27].

### D. Antibacterial Test against Escherichia coli

Prior to the bacterial test, the Nutrient Agar medium was made by weighing 2.8 g of NA media and dissolved in 100 mL of distilled water, then heated on a magnetic stirrer until homogeneous, then sterilized in an autoclave at 121°C for 1 hour. to prevent the growth of unwanted microorganisms. After sterilization, the media can be poured aseptically into sterile petri dishes for use. Before pouring the media, wait until it is lukewarm ( $\pm 40^{\circ}\text{C}$ ), then leave it at room temperature until the media solidifies completely. This was followed by a bacterial test in which the mixed sample was prepared and weighed with a weight of 0.2 g each, then a sample of Semen-ZnO weighing 0.2 grams was put into a falcon tube followed by 1 ml of a sample of Escherichia coli bacteria and then vortexed for several minutes to directly contact the bacteria with the Cement-ZnO composite [28], [29].

This is followed by a gradual dilution that aims to reduce the number of microbes suspended in the liquid. Furthermore, 1 ml of the diluted sample was poured into the media using the Spread Plate method and then incubated for 2x24 hours at room temperature. Evaluation/calculation of the number of colonies was carried out using the TPC (Total Plate Count) method with the help of a colony counter, the formula equation:

$$\left(\frac{\text{cfu}}{\text{ml}}\right) = \frac{(\text{no of colonies}) \times \text{total dilution factor}}{\text{the volume of culture plated}} \quad (1)$$

### E. XRD Instrument Sample Characterization

Characterization results of the ZnO synthesis and Cement-ZnO were carried out by the way it worked; namely, 2 X-ray beams with identical wavelengths and phases hit the solid sample, thus forming an angle with the atomic plane. Different atoms distort these X-rays, which causes the refracted beams to interact. In a certain direction, the interference is conductive. In this study, the XRD instrument aims to determine the type of crystal formed in ZnO and the type of mineral in cement, in addition to obtaining crystal size data on ZnO using the equation:

$$d = \frac{k\lambda}{\beta \cdot \cos\theta} \quad (2)$$

where the wavelength of the incident X-ray beam, d, the crystal size in nanometers, K, the Scherrer constant, and the entire width at half the maximum intensity of the reflection peak [30], [31].

### F. SEM Instrument Sample Characterization

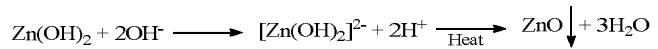
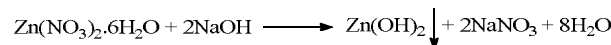
The ZnO-cement sample was characterized by a working method; namely, the electrons from the gun contained in the

SEM were directed by a magnetic lens to the sample and then received back by the secondary backscatter detector to produce morphological and topographical image information of the sample [32], [33].

## III. RESULT AND DISCUSSION

### A. ZnO Synthesis

Pure ZnO powder is produced from a mixture of ZnO nitrate hexahydrate with 0.2 M NaOH and the addition of NaOH with a maintained pH of 12. Adding NaOH separates ZnO from nitrate to form Zinc Hydroxide and Sodium Nitrate. Then, the solution is filtered for cleaning purposes. Alternatively, the separation of solid particles from a solution/fluid by passing them through a filtering medium or septum that holds the solids in place. The solid formed was dropped by drops of acetone, which aims to remove nitrate in ZnO, and was occasionally given aquabides to clean the impurities, and was baked for 5 hours with the following reaction:



A white powder was produced after filtering and washing the precipitate many times with distilled water and then acetone, producing 3.2 grams of pure ZnO powder.

### B. Mixing Process of ZnO powder and Portland Cement

Adding small amounts of nanoparticles and functional qualities like self-sensing, self-healing, and antibacterial activities dramatically influences cement-based composites' mechanical characteristics and durability. By solving intermolecular processes, the sonication process quickens the disintegration of a substance, resulting in the formation of nanoparticles. The sample was subjected to sonication with and without UV light, using a 30-watt UV light with a maximum wavelength of 365 nm and a light intensity of 144 W/m<sup>2</sup>.

According to the relative importance of photoactivation (ROS generation) and particle dissolution (including the capacity to accelerate photo-dissolution) in determining the toxicity of ZnO nanoparticles under UV radiation, UV radiation aids in speeding up the dissolution of ZnO nanoparticles. To help understand the function of ROS formation and dissolution in ZnO toxicity, the dissolution of these nanoparticles under various conditions was studied in terms of time. On the other hand, the antibacterial activities of ZnO without UV light or a light source stemmed from Zn<sup>2+</sup> ions released in water [34], [35].

On the utilized catalyst, UV light comprises photons that are helpful in the process of electron excitation from the valence band to the conduction band. If the electrons in the catalyst have sufficient energy to transition from a lower energy (valence band) to a higher energy (conduction band), they will become excited. A hydroxide radical is created when a photocatalyst interacts with a water molecule. This occurs because the electrons in both bands are unstable due to one valence band electron moving to the conduction band.

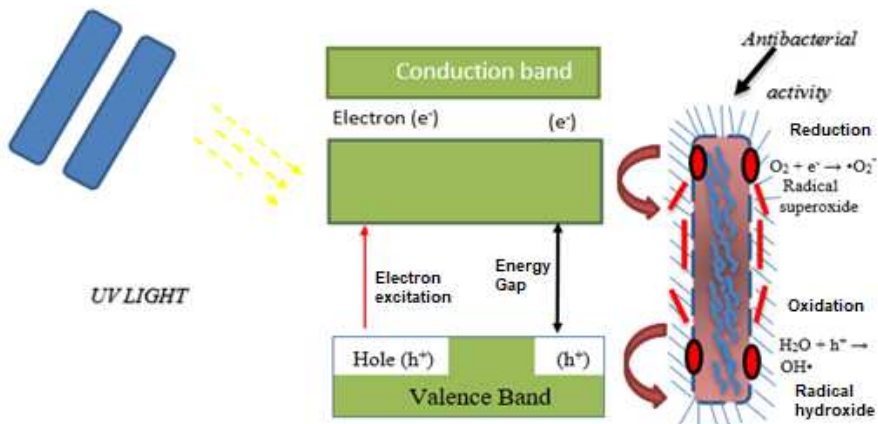


Fig. 2 ROS Mechanism

Electrons in the valence band will interact directly with water molecules to form hydroxide ions radicals while electrons in the conduction band react first with oxygen so that they will form superoxide radical anions, which in turn produce ROS from ZnO nanoparticles which are smaller than the pores bacteria will penetrate and destroy the bacterial cell wall [36], [37].

#### C. Application of Semen-ZnO against Escherichia coli bacteria with UV light

After forming a composite between Cement-ZnO, which has previously been varied with variations of 0%, 1%, 3%, and 5%, the resulting product is applied to bacteria, which aims to see the effectiveness of the product in evaluating bacteria, the following table presents the results of bacterial evaluation to the sample.

TABLE III  
RESULT OF ANTIBACTERIAL APPLICATION WITH UV LIGHT

No.	Cement-ZnO variation	No. of Colonies	(CFU/ml)
1.	0%	285	$2.85 \times 10^6$
2.	1%	203	$2.03 \times 10^6$
3.	3%	109	$1.09 \times 10^6$
4.	5%	48	$0.48 \times 10^6$

#### Percentage of E.Coli Survival on ZnO-Cement Composite with the Help of UV Light

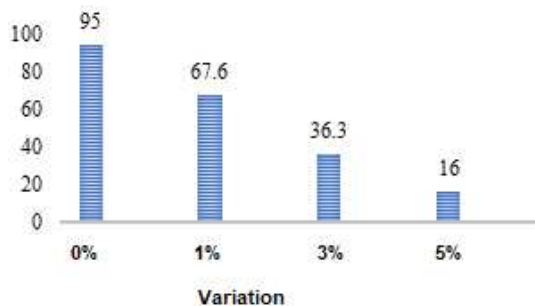


Fig. 3 The curve of survival percentage of Cement-ZnO composite against *E.coli* with UV light

The results obtained in cement with a variation of 0% ZnO obtained the amount of bacterial contamination of  $2.85 \times 10^6$ , which can be said to be on the threshold with a maximum total colony of 300, at a variation of 1% obtained the amount of microbial contamination of  $2.03 \times 10^6$ , it can be assumed that the addition of variations resulted in the

value of bacterial survival decreases, then in the 3% variation, the amount of microbial contamination is  $1.09 \times 10^6$ , this shows that the survival of bacteria is decreasing, the last variation is 5%, the data on the amount of microbial contamination is  $0.48 \times 10^6$ .

From the curve, it can be concluded that the level of bacterial life in colony-forming units per volume (CFU/ml) of *Escherichia coli* with variations in ZnO with the help of UV light. With the added variation of ZnO, the survival rate of bacteria decreased. From the smallest variation of 0% to the largest variation of 5%, a significant decrease was experienced.

#### D. Application of Cement-ZnO against Escherichia coli bacteria without UV Light

The sonication process was carried out on Cement-ZnO without the help of UV light. The beaker containing the Cement-ZnO composite was coated with aluminum foil to prevent contact with outside light so that the evaluation results were obtained in Table 4 below.

TABLE IV  
RESULT OF ANTIBACTERIAL APPLICATION WITHOUT UV LIGHT

No.	Cement-ZnO variation	No. of Colonies	(CFU/ml)
1.	0%	285	$2.85 \times 10^6$
2.	1%	203	$2.03 \times 10^6$
3.	3%	109	$1.09 \times 10^6$
4.	5%	48	$0.48 \times 10^6$

#### Percentage of E.Coli Survival on ZnO-Cement Composite without the Help of UV Light

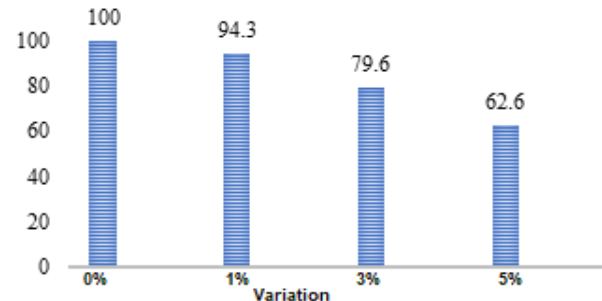


Fig. 4 *E.coli* survival percentage curve for Cement-ZnO composite without UV light

The results obtained in cement with a variation of ZnO 0%, the amount of microbial contamination that cannot be calculated/undefined, it can be said that this number exceeds the limit with a maximum total colony of 300, at a variation of 1% the amount of bacterial contamination is  $2.83 \times 10^6$ . It can be assumed that the addition of the ZnO variation resulted in a decrease in the survival value of the bacteria, then at the 3% variation, the amount of microbial contamination was  $2.39 \times 10^6$ . This indicates that the survival of the bacteria was decreasing. With the added variation of ZnO, it was found that the bacterial survival rate decreased. But not too significant. The decrease was not too significant, going from the smallest variation of 0% to the largest variation of 5%. This was because it was without the help of UV light.

#### E. XRD Instrument Characterization

The characteristic test of Cement-ZnO aims to determine the shape or type of ZnO crystals found in Portland Cement. On the other hand, it is necessary to know the size of the nanoparticles of ZnO itself contained in Portland Cement.

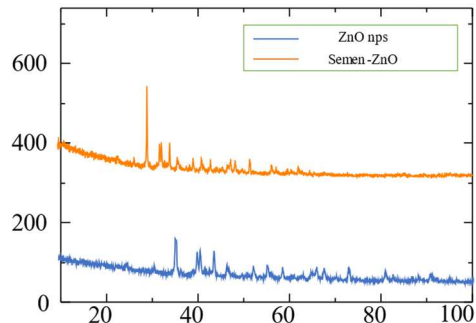
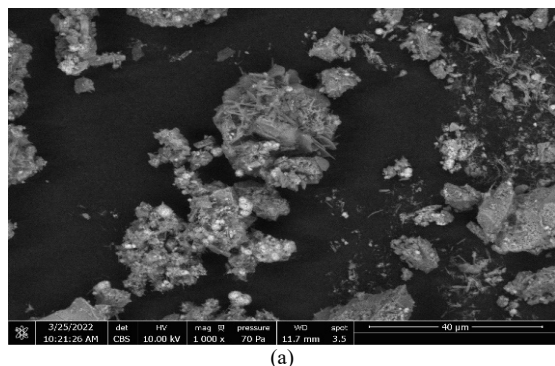


Fig. 5 XRD Pattern of Cement-ZnO

In the XRD results, the ZnO crystal form is hexagonal wurtzite which is proven by the field by confirming the high purity properties of the synthesized powder, and the structure results are almost the same as in previous studies [38], [39], where the peaks were found at angles of  $32.769^\circ$ ,  $34.2976^\circ$ ,  $36.0389^\circ$ ,  $39.417^\circ$ ,  $41.3164^\circ$ , and  $43.1495^\circ$  with hkl values  $(1\ 0\ 0)$ ,  $(0\ 0\ 2)$ ,  $(1\ 0\ 1)$ ,  $(1\ 0\ 3)$ ,  $(1\ 1\ 2)$ , and  $(2\ 0\ 1)$ .



(a)

Fig. 6 Cement ZnO Morphology

#### IV. CONCLUSION

The effect of adding ZnO to Portland Cement with the help of UV light resulted in a significant decrease in bacterial

The sharpness of the XRD spectrum graph is related to the quality of its crystallinity. The peak sharpness is also related to the curve's width or what is commonly referred to as the full width at half maximum FWHM (full-width half maximum). The FWHM value is related to the size of the crystal diameter. The larger the FWHM, the smaller the crystal diameter obtained [40], [41].

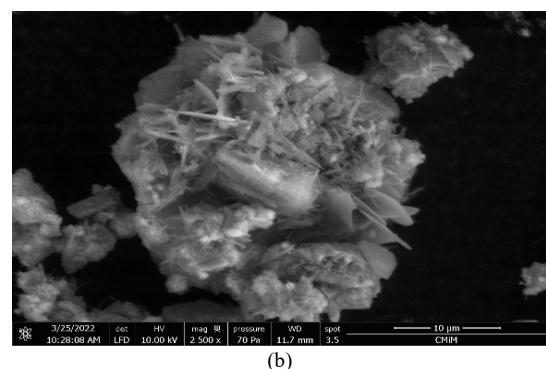
TABLE V  
ZNO CRYSTALLINE SIZE CALCULATION

Sample	Theta 2θ (°)	F.W.H.I.M. (°)	Sample Crystalline Size (nm)
Pure ZnO Powder	32.7690	0.3070	26.95803
	34.2976	0.3070	27.08113
	36.0389	0.4093	20.41056
	39.4170	0.3070	27.48736
	41.3164	0.6140	13.82768
	43.1495	0.3070	27.82674

The results of the crystal diameter measurement can be shown in Table 5. It is known that based on the results of calculations using the Debye-Scherrer formula, the crystalline size of ZnO powder obtained nanoparticle size average is 23,483 nm.

#### F. SEM Instrument Characterization

The morphology of the cement-ZnO composite (5%). At 1000x magnification, Figure 6(a) shows a sample of white cement. The images reveal that the white cement has a porous and heterogeneous structure. Figure 6(b) shows two types of morphology; one sample of white cement is similar to Figure 6(a), and the other is similar in structure to a needle or rod. The needle/rod structure is made of ZnO, which the researchers used as a cement filler or material. The microstructure of Figure 6(b) reveals that the ZnO needles/rods are solidly embedded in the white cement, and in the image reveals that the micro/nanostructure of ZnO is typical tubular microstructure/nanotubes have a hexagonal shape. The brightness contrast between the middle and the edges indicates the tube structure is hollow, under the SEM results, which can be drawn that the appearance of the hexagonal-shaped ZnO material was found [42]–[44].



(b)

survival, but without UV light, the survival of bacteria also decreased but not significantly. The results of the synthesis of ZnO were characterized by XRD formed hexagonal wurtzite crystals with peaks formed at angles of  $32.769^\circ$ ,  $34.2976^\circ$ ,

36.0389°, 39.417°, 41.3164°, and 43.1495°. The ZnO-cement composite (%) was successfully created, as seen from the SEM images, and XRD examination revealed no interaction between ZnO and white cement in the composite. In the ZnO-cement (%), no further phase development, absorption, or bonding was seen.

#### ACKNOWLEDGMENT

We express our gratitude to the Ministry of Education, Culture, Research, and Technology of the Republic of Indonesia, as well as the Institute for Research and Community Services of Universitas Negeri Padang under Penelitian Pusat/Kelompok Riset Scheme Project Number 1753/UN35.13/LT/2022

#### REFERENCES

- [1] L. Li, Y. Wei, Q. Feng, F. Liu, B. Liu, and B. Pu, "A Review : Progress in Molecular Dynamics Simulation of Portland Cement (Geopolymer) - Based Composites and the," 2023, doi:10.3390/buildings13071875.
- [2] S. N. Zailan *et al.*, "Potential Applications of Geopolymer Cement-Based Composite as Self-Cleaning Coating: A Review," *Coatings*, vol. 12, no. 2, 2022, doi: 10.3390/coatings12020133.
- [3] J. Zhu *et al.*, "Revealing the substitution preference of zinc in ordinary Portland cement clinker phases: A study from experiments and DFT calculations," *J. Hazard. Mater.*, vol. 409, no. October, p. 124504, 2021, doi: 10.1016/j.jhazmat.2020.124504.
- [4] M. Kumar, M. Bansal, and R. Garg, "An overview of beneficiary aspects of zinc oxide nanoparticles on performance of cement composites," *Mater. Today Proc.*, vol. 43, no. xxxx, pp. 892–898, 2020, doi: 10.1016/j.matpr.2020.07.215.
- [5] J. da S. Andrade Neto, A. G. De la Torre, and A. P. Kirchheim, "Effects of sulfates on the hydration of Portland cement – A review," *Constr. Build. Mater.*, vol. 279, pp. 1–40, 2021, doi: 10.1016/j.conbuildmat.2021.122428.
- [6] Y. Zhou *et al.*, "Hydration and Fractal Analysis on Low-Heat Portland Cement Pastes Using Thermodynamics-Based Methods," *Fractal Fract.*, vol. 7, no. 8, pp. 1–28, 2023, doi: 10.3390/fractfract7080606.
- [7] D. L. N. B. Jayawardane, U. UPAS, W. WMNR, and P. CK, "Physical and Chemical Properties of Fly Ash based Portland Pozzolana Cement," *Civ. Eng. Res. Exch. Symp.* 2012, pp. 8–11, 2012, doi: <http://dl.lib.mrt.ac.lk/handle/123/8931>.
- [8] N. L. Mai, N. H. Hoang, H. T. Do, M. Pilz, and T. T. Trinh, "Elastic and thermodynamic properties of the major clinker phases of Portland cement: Insights from first principles calculations," *Constr. Build. Mater.*, vol. 287, 2021, doi: 10.1016/j.conbuildmat.2021.122873.
- [9] C. Zagaglia, M. G. Ammendolia, L. Maurizi, M. Nicoletti, and C. Longhi, "Urinary Tract Infections Caused by Uropathogenic Escherichia coli Strains—New Strategies for an Old Pathogen," *Microorganisms*, vol. 10, no. 7, pp. 1–12, 2022, doi: 10.3390/microorganisms10071425.
- [10] I. Klapiszewska, A. Parus, Ł. Ławniczak, T. Jasionowski, Ł. Klapiszewski, and A. Śłosarczyk, "Production of antibacterial cement composites containing ZnO/lignin and ZnO-SiO<sub>2</sub>/lignin hybrid admixtures," *Cem. Concr. Compos.*, vol. 124, no. March, 2021, doi: 10.1016/j.cemconcomp.2021.104250.
- [11] B. A. Dehkordi, M. R. Nilforoushan, N. Talebian, and M. Tayebi, "A comparative study on the self-cleaning behavior and antibacterial activity of Portland cement by addition of TiO<sub>2</sub>and ZnO nanoparticles," *Mater. Res. Express*, vol. 8, no. 3, 2021, doi: 10.1088/2053-1591/abef41.
- [12] F. E. M. Mostafa *et al.*, "Analyzing the Effects of Nano-Titanium Dioxide and Nano-Zinc Oxide Nanoparticles on the Mechanical and Durability Properties of Self-Cleaning Concrete," 2023, doi:10.3390/ma16216909.
- [13] Hardeli, A. Indra, and Rahadian, "Preparation of dye sensitized solar cell (DSSC) using isolated anthocyanin fromfruit sat (melastomamalabathricum l) dicopimented with salicylic acid as dye," *J. Phys. Conf. Ser.*, vol. 1317, no. 1, 2019, doi: 10.1088/1742-6596/1317/1/012028.
- [14] R. Zainul, "Effect of temperature and particle motion against the ability of ZnO semiconductor photocatalyst in humic acid," *Der Pharm. Lett.*, vol. 8, no. 15, pp. 120–124, 2016.
- [15] R. Zainul, "Determination of the half-life and the quantum yield of ZnO semiconductor photocatalyst in humic acid," *Der Pharm. Lett.*, vol. 8, no. 15, pp. 176–179, 2016.
- [16] R. Verma, S. Pathak, A. K. Srivastava, S. Prawer, and S. Tomljenovic-Hanic, "ZnO nanomaterials: Green synthesis, toxicity evaluation and new insights in biomedical applications," *J. Alloys Compd.*, vol. 876, p. 160175, 2021, doi: 10.1016/j.jallcom.2021.160175.
- [17] A. Fatima *et al.*, "Zinc Oxide Nanoparticles Significant Role in Poultry and Novel Toxicological Mechanisms," *Biol. Trace Elem. Res.*, pp. 1–35, 2023, doi: 10.1007/s12011-023-03651-x.
- [18] D. Rahmadiawan *et al.*, "Enhanced UV blocking, tensile and thermal properties of bendable TEMPO-oxidized bacterial cellulose powder-based films immersed in PVA/Uncaria gambir/ZnO solution," *J. Mater. Res. Technol.*, vol. 26, pp. 5566–5575, 2023, doi: 10.1016/j.jmrt.2023.08.267.
- [19] R. Zainul *et al.*, "Zinc/aluminium–quinclorac layered nanocomposite modified multi-walled carbon nanotube paste electrode for electrochemical determination of bisphenol A," *Sensors (Switzerland)*, vol. 19, no. 4, 2019, doi: 10.3390/s19040941.
- [20] M. A. Irshad *et al.*, "Synthesis and characterization of titanium dioxide nanoparticles by chemical and green methods and their antifungal activities against wheat rust," *Chemosphere*, vol. 258, p. 127352, 2020, doi: 10.1016/j.chemosphere.2020.127352.
- [21] N. Babayevska *et al.*, "ZnO size and shape effect on antibacterial activity and cytotoxicity profile," *Sci. Rep.*, vol. 12, no. 1, pp. 1–13, 2022, doi: 10.1038/s41598-022-12134-3.
- [22] I. H. Ifijen, M. Maliki, and B. Anegbe, "Synthesis, photocatalytic degradation and antibacterial properties of selenium or silver doped zinc oxide nanoparticles: A detailed review," *OpenNano*, vol. 8, no. July, p. 100082, 2022, doi: 10.1016/j.onano.2022.100082.
- [23] V. P. Singh, K. Sandeep, H. S. Kushwaha, S. Powar, and R. Vaish, "Photocatalytic, hydrophobic and antimicrobial characteristics of ZnO nano needle embedded cement composites," *Constr. Build. Mater.*, vol. 158, pp. 285–294, 2018, doi: 10.1016/j.conbuildmat.2017.10.035.
- [24] I. Klapiszewska *et al.*, "Influence of zinc oxide particles dispersion on the functional and antimicrobial properties of cementitious composites," *J. Mater. Res. Technol.*, vol. 24, pp. 2239–2264, 2023, doi: 10.1016/j.jmrt.2023.03.131.
- [25] A. Babaei, M. Ghazavi, and N. Ganjian, "Experimental investigation of nano-ZnO effect on mechanical properties of cemented clayey sand," *Bull. Eng. Geol. Environ.*, vol. 81, no. 1, pp. 1–16, 2022, doi: 10.1007/s10064-022-02568-4.
- [26] F. Amor, M. Baudys, Z. Racova, L. Scheinherrová, L. Ingrisova, and P. Hajek, "Contribution of TiO<sub>2</sub> and ZnO nanoparticles to the hydration of Portland cement and photocatalytic properties of High Performance Concrete," *Case Stud. Constr. Mater.*, vol. 16, no. February, 2022, doi: 10.1016/j.cscm.2022.e00965.
- [27] J. Li, G. Cheng, S. Huang, and P. Lian, "Effect of ZnO on the whiteness of white Portland cement clinker," *Cem. Concr. Res.*, vol. 143, no. December 2020, p. 106372, 2021, doi: 10.1016/j.cemconres.2021.106372.
- [28] D. E. Navarro-López *et al.*, "Nanocomposites based on doped ZnO nanoparticles for antibacterial applications," *Colloids Surfaces A Physicochem. Eng. Asp.*, vol. 652, no. May, 2022, doi: 10.1016/j.colsurfa.2022.129871.
- [29] V. P. Singh, R. Vaish, and E. S. Yousef, "A Review on Cement-Based Composites for Removal of Organic/Heavy Metal Contaminants from Water," *Catalysts*, vol. 12, no. 11, 2022, doi: 10.3390/catal12111398.
- [30] M. Parashar, V. K. Shukla, and R. Singh, "Metal oxides nanoparticles via sol–gel method: a review on synthesis, characterization and applications," *J. Mater. Sci. Mater. Electron.*, vol. 31, no. 5, pp. 3729–3749, 2020, doi: 10.1007/s10854-020-02994-8.
- [31] S. Agrohiya *et al.*, "Nickel Doped Zinc Oxide Thin Films for Visible Blind Ultraviolet Photodetection Applications," *ECS Sensors Plus*, vol. 1, no. 4, p. 043601, 2022, doi: 10.1149/2754-2726/ac973f.
- [32] X. Li, J. Li, Z. Lu, and J. Chen, "Properties and hydration mechanism of cement pastes in presence of nano-ZnO," *Constr. Build. Mater.*, vol. 289, p. 123080, 2021, doi: 10.1016/j.conbuildmat.2021.123080.
- [33] A. M. Mocioiu *et al.*, "Self-Cleaning and Antibacterial Properties of the Cement Mortar with ZnO/Hydroxyapatite Powders," *Inorganics*, vol. 10, no. 12, 2022, doi: 10.3390/inorganics10120241.
- [34] I. Klapiszewska, A. Kubiak, A. Parus, M. Janczarek, and A. Śłosarczyk, "The In Situ Hydrothermal and Microwave Syntheses of Zinc Oxides for Functional Cement Composites," *Materials (Basel.)*, vol. 15, no. 3, 2022, doi: 10.3390/ma15031069.

- [35] C. Pushpalatha *et al.*, "Zinc Oxide Nanoparticles: A Review on Its Applications in Dentistry," *Front. Bioeng. Biotechnol.*, vol. 10, no. May, pp. 1–9, 2022, doi: 10.3389/fbioe.2022.917990.
- [36] J. Ye, B. Li, M. Li, Y. Zheng, S. Wu, and Y. Han, "Formation of a ZnO nanorods-patterned coating with strong bactericidal capability and quantitative evaluation of the contribution of nanorods-derived puncture and ROS-derived killing," *Bioact. Mater.*, vol. 11, no. August 2021, pp. 181–191, 2022, doi: 10.1016/j.bioactmat.2021.09.019.
- [37] M. Godoy-Gallardo *et al.*, "Antibacterial approaches in tissue engineering using metal ions and nanoparticles: From mechanisms to applications," *Bioact. Mater.*, vol. 6, no. 12, pp. 4470–4490, 2021, doi: 10.1016/j.bioactmat.2021.04.033.
- [38] M. Xin, "Crystal Structure and Optical Properties of ZnO:Ce Nano Film," *Molecules*, vol. 27, no. 16, pp. 1–9, 2022, doi: 10.3390/molecules27165308.
- [39] M. Benamara, A. Ly, S. Soltani, M. Essid, and H. Dahman, "RSC Advances Enhanced detection of low concentration volatile organic compounds using advanced doped zinc oxide sensors," pp. 30230–30242, 2023, doi: 10.1039/d3ra03143h.
- [40] T. Hashimoto, E. R. Letts, and D. Key, "Progress in Near-Equilibrium Ammonothermal (NEAT) Growth of GaN Substrates for GaN-on-GaN Semiconductor Devices," *Crystals*, vol. 12, no. 8, 2022, doi: 10.3390/cryst12081085.
- [41] K. Wijaya *et al.*, "Recent Trends and Application of Nanomaterial Based on Carbon Paste Electrodes: A Short Review," *Evergreen*, vol. 10, no. 3, pp. 1374–1387, 2023, doi: 10.5109/7151686.
- [42] C. Ortega-Nieto, N. Losada-Garcia, D. Prodan, G. Furtos, and J. M. Palomo, "Recent Advances on the Design and Applications of Antimicrobial Nanomaterials," *Nanomaterials*, vol. 13, no. 17, 2023, doi: 10.3390/nano13172406.
- [43] T. Iqbal, A. Raza, M. Zafar, S. Afsheen, I. Kebaili, and H. Alrobei, "Plant-mediated green synthesis of zinc oxide nanoparticles for novel application to enhance the shelf life of tomatoes," *Appl. Nanosci.*, vol. 12, no. 2, pp. 179–191, 2022, doi: 10.1007/s13204-021-02238-z.
- [44] M. H. Aleinawi, A. U. Ammar, M. Buldu-Akturk, N. S. Turhan, S. Nadupalli, and E. Erdem, "Spectroscopic Probing Of Mn-Doped ZnO Nanowires Synthesized via a Microwave-Assisted Route," *J. Phys. Chem. C*, vol. 126, no. 8, pp. 4229–4240, 2022, doi: 10.1021/acs.jpcc.2c00009.